A Comparative Study of Fiber Optic Gyroscopes

Journal of Physics: Conference Series **2847** (2024) 012005 doi:10.1088/1742-6596/2847/1/012005

A Comparative Study of Fiber Optic Gyroscopes

Mohamed N. Shalaby[1,†,*] and Ahmed H. Elghandour[2,†]

[1] Engineering Physics Department, Military Technical College, Cairo, Egypt
[2] Communication Department, Military Technical College, Cairo, Egypt

Email : Mohamedshalaby5599@mtc.edu

† These authors contributed equally to this work.

Abstract. Inertial Navigation Systems (INS) are integral to modern technology, yet their significance often goes unnoticed. Key to an INS are Gyroscopes, which detect rotation rates. Initially mechanical, they became outdated with advancing technology, prompting the development of Optical Gyroscopes. This paper explores various Gyroscope technologies, emphasizing Fiber Optic Gyroscopes, and delves into their operational theory and associated challenges.

1. Introduction

Inertial Navigation Systems (INS) quietly drives our modern world by being one of the most important basic parts of all modern systems. INS use Gyroscopes and accelerometers to understand complex three-dimensional movement. Wherever there is no way to receive any guidance signals, INS unofficially steers planes [1,2], submarines, and spaceships to keep them in perfect sync. By adding a Global Positioning System (GPS) to an inertial navigation system (INS) increase guidance and navigation process accuracy and resolution by filling their individual limitations [3] [4].

The rotation angle must be precisely determined in order for the control system to function properly and ensure safety. Even, other onboard sensors like Radar, Lidar, or cameras can identify this angle, but their accuracy and dependability are greatly reliant on the algorithm utilized, environmental variables, and several other factors which are not affecting INS systems.

As Gyroscopes are critical components of INS, due to its rule in measuring rotation rates and, rotations. Initially, Mechanical Gyroscopes were adequate for this purpose [5], however, their evolution encountered various challenges, which forced researchers to work in finding alternatives. Which lead them to develop Optical Gyroscopes, such as Ring Laser Gyroscopes [RLGs] [6], Fiber Optic Gyroscopes [FOGs] [7], and Micro-Electro-Mechanical Gyroscopes [MEMS] [8], as viable alternatives to Mechanical Gyroscopes.

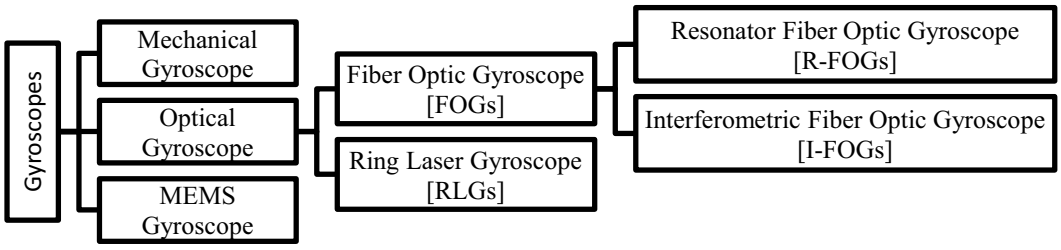

Figure 1. Types of Gyroscopes

In this present work we will introduce a survey on all types of Gyroscopes as shown in figure 1, and we while pointing out their weaknesses and talking about how to improve them. Also we will review thoroughly at Optical Gyroscopes, focusing on FOGs in particular.

2. Mechanical Gyroscopes

A Mechanical Gyroscopes is mainly a rotating mass that spins around its axis [9] . When the mass rotates, it tries to stay in the same position and beats off outside attempts to change its direction. This process, which was first suggested by the scientist Léon Foucault in 1852 while he was studying how the Earth spins, shows that it is stable. Putting the Gyroscope on gimbals as shown in figure 2 [10], which let it move freely along three spatial axes, makes sure that the spinning axis stays in the same position even if the direction of movement changes [11].

In the past, Mechanical Gyroscopes were useful for navigation, control, and guiding. However, as these fields have grown, they became less useful they can't not match the new developed requirements for the modern advances. With all of their moving parts, Mechanical Gyroscopes were either huge in size or heavy in weight or both of those. Their need to warming up was complicated and took a long time, which made it hard to rely on and cost too much [12,13].

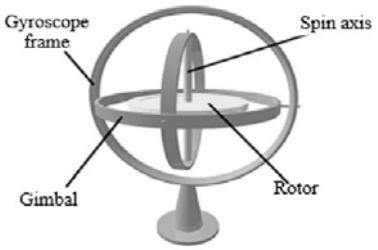

Figure 2. Mechanical Gyroscopes

3. Micro-Electro-Mechanical System [MEMS] Gyroscopes

Silicon-based MEMS inertial sensors have gained popularity and are readily available in the market. Among these, MEMS Gyroscopes stand out for their small size, weight, and low cost, making them appropriate for a wide range of applications, from high-performance navigation systems to consumer electronics. The best MEMS Gyroscopes available commercially have an Angular Random Walk (ARW) of 0.09 degrees per hour, a resolution of 20 degrees per hour, and bias stability that ranges from 5 to 10 degrees per hour.

Over the last decade, a lot of study has been done to enhance the MEMS Gyroscopes performance. For instance, the European Space Agency started a project in 2005 to make a cheap Gyroscope that could be used in space. The Gyroscope had to have an ARW of less than 0.2 degrees per hour and bias stability between 5 and 10 degrees per hour. With an ARW of 0.04 degrees per hour and bias stability ranging from 10 to 20 degrees per hour, the current prototypes from this study look like they will work well.

Recent advances include a prototype of a tuning fork MEMS Gyroscopes based on a Silicon-on-Insulator substrate with a remarkable ARW of 0.003 degrees per hour and bias stability of 0.15 degrees per hour. Despite having lower performance than FOGs and He-Ne RLGs, MEMS Gyroscopes are both cost-effective and small size, making them an appealing choice for a variety of applications [14,15].

MEMS Gyroscopes usually use mechanical parts that vibrate as sensors to measure angular speed. Their design doesn't have any moving parts that need bearings, which makes it easier in reducing the size using MEMS production methods. Coriolis acceleration, which is a force that seems to be acting on a spinning frame of reference and is related to angular velocity, is what these Gyroscopes depend on to move energy from one vibrating mode to another [16–19].

In the last few years several studies were conducted at UCBerkeley to combine both signal processing and control on a chip to create a dual-axis Gyroscope, and to improve both manufacturing and performance by introducing a design with multi-degree of freedom. Juneau, Pisano, and Smith used a rotating disk that detects rotation in two orthogonal axes to created a surface-micromachined dual-axis Gyroscope.

Since 1996, Clark, Howe, and Horowitz have been working on the z-axis motion rate Gyroscope. The tool has a trans-resistance amplifier and interdigitated comb fingers for measuring differences in the sense mode [20,21]. Mochida, Tamura, and Ohwada from the Murata, Yokohama R&D Center in 1999 released two designs for micro-machined Gyroscopes. One design had a simple structure that could be used to compare it to others, while the other for the drive and detection modes it apply different beams. By cutting off the connection between the drive and sense states, this separation improved the resolution.

The Georgia Institute of Technology also did a lot of work to learn more about MEMS Gyroscopes. They managed to made the Matched-Mode Tuning Fork Gyroscope (M2-TFG) in 2006. With an electric comb drive, it moved the proof masses along the x-axis. A sensitive sensor in the y-axis told it when the z-axis turned [22,23]. Sharma studied the M2-TFG more and came up with a closed-loop circuit based on a trans-impedance amplifier with a 104 dB dynamic range that can keep the matched-mode.

Trusov et al. worked on two projects at the University of California from 2009 to 2011. The first was a tuning fork-based z-axis MEMS Gyroscope device. The second was a brand-new dual-mass vibratory MEMS z-axis rate Gyroscope that enhanced the mechanical vibratory modes [24]. Both Old Dominion University and the University of Utah worked together on the M2-TFG concept to improve its performance. There is a multiple beam tuning fork Gyroscope that Wang et al. showed. It has a Q-factor of 255,000 in drive mode and 103,000 in sense mode at 15.7 kHz [25].

In 2012, Tsai et al. created a MEMS Gyroscopes that was twice decoupled to reduce coupling between the drive-mode and sense-mode. This Gyroscope used frequencies in the 240 Hz bandwidth [26]. In 2017, Pyatishev et al. wrote about a MEMS Gyroscopes that had a drive in the shape of a comb and a bigger capacity gradient. They believed one of the most important ways to improve the comb drive performance, this was accomplished by changing its aspect ratio, which was known as its "wavy aspect ratio" [27].

4. Optical Gyroscopes

4.1 Theory of Optical Gyroscopes

The creation of Optical Gyroscopes was a direct result of advances in lasers and fibers. It was a team effort by researchers to address the constraints inherent in Mechanical Gyroscopes. By utilizing the advances in laser and fiber optic technologies, researchers tried to overcome the limitations associated with Mechanical Gyroscopes, resulting in the development and refining of Optical Gyroscopes. All Optical Gyroscopes rely on the whats know by "Sagnac effect", however the effect produces frequency shift or phase shift between two counter propagating waves.

4.1.1. Sagnac effect. The Sagnac effect, which is at the heart of most Optical Gyroscopes [5,28–31] , describes the relative phase shift between two light beams going in opposite directions along the same path within a rotating frame [32–34] . This principle, discovered by George Marc Sagnac in 1913, observes a time delay (Δt) between counter-propagating optical waves along a rotating closed route. Sagnac's mirror-based ring interferometer demonstrated a fractional fringe shift under rotation, a key-step forward in understanding this phenomenon. Michelson-Morley's research into Earth's dynamics and observations within non-inertial reference systems led to its development. This concept asserts that the phase shift between counter-propagating optical beams within a rotating ring construction is directly proportional to the setup's rotational rotation [35–38].

According to Sagnac, "At any rotating medium, there will be a phase shift between two counter-propagating beams [39], and this phase shift will depend on the rotation rate of the medium" [40]. Although, the two beams will cover the same optical distance and take the same path, However, there will be a path difference between the beams as they go since the clockwise beam will travel farther than the other if the system rotates in that way as shown in figure 2 [41,42].

The following is a simple Sagnac effect calculation utilizing a circular waveguide structure. The wave guidance shown in figure 3 is considered to be in a vacuum. At a given position on the optical beam guide, light enters and exits the loop. While, entry and exit points will follow the optical beam guide as it rotates which need time period for counter-propagating light waves to complete one loop [43].

Consider light travelling in the opposite direction the path length of the optical beam guide in a stationary situation is ℓ =2πr. However, if the optical beam guide rotates counterclockwise with angular velocity, the path length grows to [7]

$$\ell_{CCW} = \ell + \Delta\ell = 2\pi \cdot r + \Delta\ell \qquad \ell_{CW} = \ell - \Delta\ell = 2\pi \cdot r - \Delta\ell \tag{1}$$

The difference in counterclockwise (CCW) and clockwise (CW) path lengths is calculated as

$$\Delta\ell = \Omega \cdot r \cdot \tau_{CCW} \qquad \Delta\ell = \Omega \cdot r \cdot \tau_{CW} \tag{2}$$

where v=ωr is the tangential velocity of the optical beam guide (optical fiber coil), Ω is the rotation rate of the medium and C is the speed of light, the time required for the counterclockwise propagating beam to arrive at the exit point is calculated as

$$\tau_{CCW} = \frac{\ell+\Delta\ell}{c} = \frac{2\pi \cdot r+\Omega \cdot r \cdot \tau_{CCW}}{c} \tag{3}$$

Similarly, the time required for the clockwise propagating light wave to arrive at the exit point is calculated as

$$\tau_{CW} = \frac{\ell-\Delta\ell}{c} = \frac{2\pi \cdot r-\Omega \cdot r \cdot \tau_{CW}}{c} \tag{4}$$ so,

$$\tau_{CCW} = \frac{2\pi \cdot r}{c-\Omega \cdot r} = \frac{\ell}{c-v} \tag{5}$$

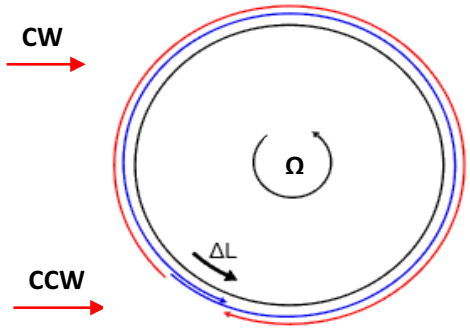

Figure 3. Change of path length of CW and CCW beams due to rotation

$$\tau_{CW} = \frac{2\pi \cdot r}{c + \Omega \cdot r} = \frac{\ell}{c+v} \tag{6}$$

Thus, the traveling time difference ($\Delta\tau$) between these two wave can be calculated by

$$\Delta\tau = \tau_{CCW} - \tau_{CW} = \frac{\ell}{c-v} - \frac{\ell}{c+v} = 2\pi \cdot r \cdot \left(\frac{2v}{c^2-(v)^2}\right) = \frac{4\pi \cdot r \cdot v}{c^2 \cdot \left(1-\left(\frac{v}{c}\right)^2\right)} \tag{7}$$

as $v=\Omega.r << c$ is rather small compared with the speed of light c, so traveling time difference simplifies to

$$\Delta\tau = \tau_{CCW} - \tau_{CW} \approx \frac{4\pi \cdot r \cdot v}{c^2} = \frac{4\pi \cdot r^2}{c^2} \cdot \Omega = \frac{4a}{c^2} \cdot \Omega = \frac{2r \cdot \ell}{c^2} \cdot \Omega \tag{8}$$

and $a = \pi r^2$ is the area bounded by the optical fiber coil and $\Delta\ell$ is calculated as

$$\Delta\ell = \Delta\tau \cdot c = \frac{4\pi \cdot r^2}{c} \cdot \Omega = \frac{4a}{c} \cdot \Omega = 2 \cdot \frac{v}{c} \cdot \ell \tag{9}$$

The $\Delta\varphi s$ which is defined as Sagnac phase shift is calculated as

$$\Delta\phi_S = \omega \cdot \Delta\tau = 2\pi \cdot f \cdot \Delta\tau = 2\pi \cdot \frac{c}{\lambda} \cdot \Delta\tau = \frac{8\pi^2 \cdot r^2}{\lambda \cdot c} \cdot \Omega = \frac{8\pi \cdot a}{\lambda \cdot c} \cdot \Omega = \frac{4\omega \cdot a}{c^2} \cdot \Omega \tag{10}$$

where $\omega = 2\pi f$ is angular frequency and $f = \frac{c}{\lambda}$ is the frequency of light wave.

Thus, for Fiber Optic Gyroscopes composed of N-turns Substituting coil length $L=2\pi rN$ and coil diameter $D=2R$, so

$$\Delta\phi_S = \frac{4\omega \cdot aN}{c^2} \cdot \Omega = \frac{42\pi C \cdot aN}{\lambda c^2} \cdot \Omega = \frac{4*2\pi \cdot \pi * r * rN}{\lambda c} \cdot \Omega = \frac{2\pi LD}{\lambda C} \cdot \Omega \tag{11}$$

This result define the phase shift due to the Sagnac effect for a light of wavelength λ propagating through a coil of length L and diameter D [42,44]. $SF = \frac{2\pi LD}{\lambda C}$ Called Scale Factor which is the most important parameter for Optical Gyroscopes.

We should note that we assumed that the two beams move in free space, so this calculation at vacuum, if the light pass through the material as fiber, the Sagnac conclusion is the same at vacuum [38,45].

4.1.2. Interference of waves. Wave interference is a fundamental technique used in Optical Gyroscopes where counter-propagating waves interfere, interact, and are eventually recorded by a detector within the Gyroscope structure after traveling the length of the fiber. In the lack of rotation and hence no phase shift, the interfering waves exhibit maximum power. However, as the medium spins, the phase difference ($\Delta\phi$) between the beams causes a decrease in measured power. This shift in phase, which affects two monochromatic waves, adds to the observed power change.

That means that $\Delta\phi$ between counter propagating waves isn't measured directly, but the detected power of the interfered beams is measured after traveling through the fiber length, where the phase

shift between the two beams is deduced from the detected power as shown in equation 12, and then we can conclude the rotation rate using the Sagnac equation 11 [2,46].

$$I = \frac{I_0}{2}[1 + \cos(\Delta\phi_s)] \quad (12)$$

where I is the detected power, Io is the input intensity and Δφs is the sagnac phase shift due to rotation [47].

Also, it's clear that $\Delta\phi$ is related to the detected power at the detector by a raised cosine as any interferometer which is shown in figure 4 [48].

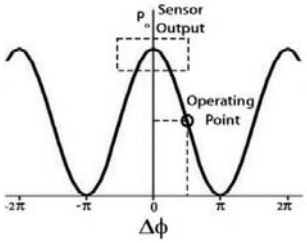

Figure 4. the relation between phase shift and detected power

4.1.3. Principle of Reciprocity. The Sagnac effect, which results from the medium's rotation, produces a tiny phase shift by definition. As a result, it is susceptible to suppression by more prominent sources of phase shift, such as environmental influences like changing temperatures over time. To maintain measurement accuracy, it is critical to eliminate any possible sources of phase changes other than the desired rotation rate. Alternatively, if complete suppression is not possible, efforts should be devoted toward ensuring that the impact of these external elements is uniform throughout both counter-propagating beams. This rigorous technique is critical for preserving the reliability and precision of Optical Gyroscopes. This is called the Reciprocity Principle.

4.2 Types of Optical Gyroscopes

In this section, we'll discuss the different types of Optical Gyroscopes, including their operating methods, strengths, limitations, and distinguishing features. The development of Optical Gyroscopes was a direct result of advances in lasers and fibers. It was a collaborative effort by researchers to address the constraints inherent in Mechanical Gyroscopes. Using advances in laser and fiber optic technologies, researchers tried to overcome the limitations associated with Mechanical Gyroscopes, resulting in the development and refining of Optical Gyroscopes. As previously stated, all Optical Gyroscopes' operation is built on the Sagnac effect, but they differ at the result of this effect the result is frequency shift or phase shift between two counter propagating waves [49–52].

4.2.1. Ring Laser Gyroscopes [RLGs]. The Ring Laser Gyroscopes (RLG) combines optical frequency generation and rotation sensing within a laser oscillator, resulting in a ring-shaped cavity. Typically, it consists of as shown in figure 5 [12] a solid block of glass ceramic material enclosing a helium/neon laser medium. Electrodes produce gain in the lasing medium, resulting in two counter-propagating beams within the cavity. The interference of these beams produces fringe patterns that can be detected by optical detectors, with the number of fringes giving the rotation rate and direction. RLG functions as an integrating system, calculating angular displacement by counting beat frequency. The RLG, which was developed shortly after the creation of the laser, recirculates counter-propagating waves within a closed resonant channel to increase sensitivity. However, at low input rates, the RLG has lock-in owing to backscattering from poor mirrors, which can be addressed by applying a frequency bias via a piezo-electric drive.

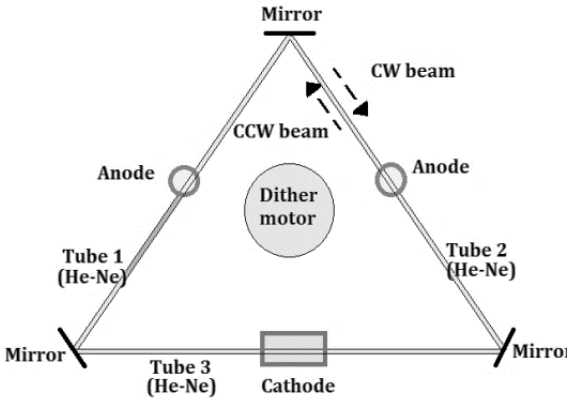

Figure 5. Ring Laser Gyroscope [RLG]

RLGs use the Sagnac phenomenon, in which the frequency changes of counter-propagating resonant modes indicates cavity rotation. RLGs, which are typically made up of a triangular glass block and a low-pressure helium-neon gas, detect angular velocity changes by altering the resonant behavior or interference patterns of the generated laser beams, as explained by the Sagnac effect [51,53].

4.2.1.1. *Advantages and disadvantages of RLGs*. RLGs were invented primarily to solve problems with Mechanical Gyroscopes. Even RLG have several limitations it also offer several advantages over Mechanical Gyroscopes, including high sensitivity, short reaction times, stability, linear output with angular rotation and tolerance to external impacts [54].

The RLG's size and weight are further issues that limit its use. Most RLGs have a solid glass optical block and a mechanical dither assembly, which add to their weight. Attempts to miniaturize the RLG resulted in a reduction in reliability. Large RLGs can operate for over 10,000 hours, whereas smaller units (with diameters of a few centimeters) only last a few hundred hours. Smaller RLGs may experience shelf-life issues due to gradual gas medium leakage, which is less noticeable in larger systems. RLGs have very high-power requirements. RLGs require high-voltage, low-current power sources to enable their lasing action [4,55]. Finally, we state that many modifications have been made for RLGs to improve their performance [56,57].

4.2.1.2. *Recent Progress in RLGs*. In the last couple of decades, significant advances in RLGs have been made. Several strategies have been offered to enhance the performance of these Gyroscope scopes. Cai and colleagues (Cai et al., 24) created strong soft magnetic alloys in 2007 that are resistant to external loads and temperature fluctuations. This advancement permitted the design of a four-mode ring laser Gyroscope with a wide temperature operating range. In 2008, Mignot and his coworkers (Mignot et al) made a big step forward when they showed that a single-frequency RLGs could work. To make this happen, the gain medium had to be a diode-pumped half-vertical-cavity semiconductor-emitting laser construction. This step made the RLGs more accurate in terms of their size [56].

In a Solid-State RLGs, Schwartz and his colleagues (Schwartz et al) were able to reduce nonlinear interactions that were caused by crystal diffusion and spatial in homogeneities. The gain crystal was shaken at 168 kHz and 0.4 m along the hollow axis, which stopped the signal at a lot of different angles[57]. In 2012, employed direct dither control without external feedback to prevent RLG lock-in. A proposed new design reduces system size and costs [58].

Unlike the typical active Gyroscope design, an innovative "passive" Gyroscope design is given, with the sensing cavity tracked by external laser beams avoids the negative lock-in effect[59]. Furthermore, it has the advantage of being built from easily available commercial components. Recently, a better calculation was made for determining the Sagnac frequency of a large square RLG while the Earth is rotating [60]. This includes changes to the gain medium and mirror dispersion, as well as the Goos-Hanchen effect in the mirrors and the refractive index of the gas in the cavity. For the study, the 16 m^2 Grossing laser at the Geodetic Observatory Wettzell was measured and its changes were worked out.

4.2.2. Fiber Optic Gyroscopes [FOGs]. Currently, two types of Fiber Optic Gyroscopes are in development: the Interferometric Fiber Optic Gyroscope (I-FOG) and the Resonant Fiber Optic Gyroscope (R-FOG).

4.2.2.1 *Resonator Fiber Optic Gyroscopes [R-FOGs].* Despite its better accuracy potential, the R-FOG has received less attention and is still in its early stages of development. R-FOGs, like RLGs, use a narrowband light source and an optical cavity made of tuned optical fibers to propagate certain frequencies of light. In the R-FOG arrangement, the fiber resonator consists of a few coiled fibers and a beam splitter. Both clockwise (CW) and counterclockwise (CCW) beams, which are normally created by the same coherent light source, enter the device via two input ports. In the absence of rotation, both beams travel the same length through the coil. However, when one beam rotates, its path length rises while the other decreases, resulting in Sagnac frequency shifts. R-FOGs, like RLGs, detect beat frequency using the equation $\Delta f = fcw - fccw$. R-FOGs, unlike RLGs, do not have a lasing medium in the resonator, hence Δf must be measured outside. This is frequently accomplished using frequency-shifting devices such as acousto-optic modulators (AOMs) to track the beam frequencies, fcw and fccw, and calculate the differential frequency.

R-FOGs have many advantages and disadvantages, they provide advantages such as short fiber lengths (5:10 m), reduced drift from temperature variations, and lower sensing coil costs. The scale factor fluctuations are decreased by employing a low coherent light source. But they also suffer from some limitations. Resonant fiber optic Gyroscope s (R-FOGs) require vital parts (coherent light source, low loss couplers, and frequency shifters) that are not commercially available and may not tolerate harsh field conditions [30,61].

4.2.2.2. *Interferometric Fiber Optic Gyroscopes [I-FOGs].* I-FOGs, the other type of FOGs, operates with a few key components, as indicated in figure 6, a light source, a 3dB coupler or splitter (splits the light into two equal beams), a fiber coil through which these beams travel one clockwise (cw), the other counterclockwise (ccw) before meeting again and heading to a detector [62]. The detector monitors the strength of the light when it recombines. This strength indicates the phase shift between the two beams, which, as Sagnac discovered, varies depending on how rapidly everything spins. In addition to these components, there is a phase modulator linked to a sine generator.

As previously discussed, this arrangement improves the Gyroscope's sensitivity by moving the zero point i.e. detected power when there is no rotation from maximum power to a point which have a maximum slope (Operating point shown in figure 3). A lock-in amplifier is another specialized device. This device functions like a detective, extracting the particular signal required to determine how quickly items are spinning. Simply, after traveling through the fiber coil in different directions, the two beams recombine at the coupler and reach the detector [62–65]. We measure the phase shift between the two beams indirectly by measuring the detected power at the detector, we can use equation 12 to calculate the phase shift between two beams, and we can use the Sagnac relation to calculate the rotation rate, which is the cause of the phase shift, as shown in equation 11 [7,66].

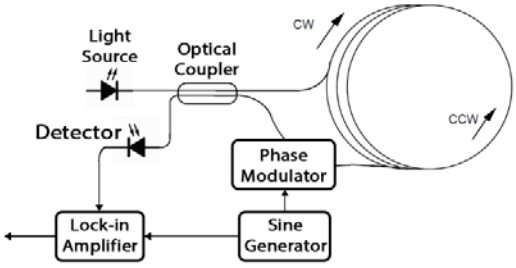

Figure 6. Interferometric Fiber Optic Gyroscope [I-FOG]

One of the great things about I-FOGs is that they're really simple in design and may be extremely compact, especially with the current fiber technology making everything smaller. I-FOGs have the appealing property that their design is almost fixed, as if the application is changed, we only change the length of the fiber coil to improve sensitivity if the application requires high sensitivity but the other components are fixed. They're also quite good at preserving power. That's why many individuals enjoy utilizing them. I-FOGs are inexpensive, compact, and consume little power. But here's the catch: they don't have as precise measurements as RLGs [65–67]. Vali and Shorthill introduced the first experimental configuration of an I-FOG in 1976. Since then, there have been significant advances in the discipline.

Cahill and Udd at McDonnel Douglas achieved closed loop operation of fiber Gyroscopes in the late 1970s by utilizing Bragg cells. The Gyroscope achieved the necessary scale factors, but the Bragg cells were bulky, difficult to interface with, and consumed high power [68].

In 1985, Thompson CSF's Arditty and Lefevre released a study on the serrodyne dual loop closure approach for closed loop operation of Fiber Gyroscope. The linear voltage ramp was replaced by a digital staircase. The step size set by the first loop closed the loop and allowed for a wide dynamic range [69]. In 1989, the fiber optics industry lacked responses for two critical assembly processes: winding the sensing coil and pigtailing the MIOC. To achieve cost targets, these processes needed to be automated. Litton automated processes by creating coil winding and pigtailing robots [5]. In 2006, the first air-core photonic-bandgap Fiber Gyroscope was introduced. The Gyroscope displayed reduced power and magnetic field dependence because the optical mode in the sensing coil passes primarily through air, which has lower Kerr, Faraday, and thermal constants than silica. In 2007, an innovative open-loop design of an I-FOG was presented, which used a single-mode optical fiber as the sensing coil and an Erbium-Doped Fiber Amplifier (EDFA) pumped with a Distributed Feedback (DFB) laser as the broadband source [70]. The Sagnac phase shift was determined using a phase tracking circuit that included an RC bandpass filter, an amplifier, and a modulator chip.

Yu et al. published an innovative concept for an I-FOG in 2009 [71] . This novel construction wanted to reduce the impact of polarization crosstalk while increasing manufacturing efficiency. In

2010, Yahalom et al. proposed a novel I-FOG. The unique design resulted in a tiny, low-cost Gyroscope with superior noise and bandwidth properties. The goal was to create an affordable sensor measuring less than 50 cm^3. In 2013, it was shown that operating an I-FOG with a laser with a broad linewidth (about 10 MHz) decreased noise to 0.058/h and bias drift to 1.1 degree/h [72]. In 2013, a 2.5 cm diameter ring was fitted with a low-noise, low-delay digital signal processor based on FPGA [73], achieving 0.67°/s bias stability over 3600 seconds. In 2013 too, Lei et al [74]. developed the first Gyroscope scope system using a current modulation approach in an external cavity laser diode. Wang et al. in 2014 introduced a dual-polarization I-FOG that requires only one coupler and no polarizer [75].

4.2.2.3. Sources of error in FOGs

4.2.2.3.1. *Backscattering errors*. Backscattering in the fiber coil has a number of negative impacts on the operation of the Gyroscope as it can occur in a distributed manner, as with Rayleigh scattering, or at localized locations, such as splices and other optical interfaces. We'll refer to these as "back reflections." Rayleigh scattering is a feature of fiber material that cannot be easily removed, however back reflections can be reduced by employing better splicing processes or angled interfaces. Along with Rayleigh scattering, random geometric changes at the core-cladding junction cause scattering to spread out. Due to thermodynamic principles, these alterations are limited and cannot be totally undone.

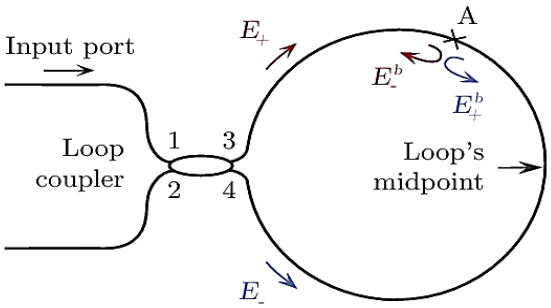

Figure 7. Effect of a single scatterer in the FOG coil

Figure 7 [2] depicts the influence of a single scatterer situated within the fiber coil [11]. The singular scatterer generates two extra incidental fields within the coil, denoted as E_+^b and E_-^b in figure 7. When these incidental fields escape, they take quite different optical paths than the primary fields and each other, this change in optical pathways represents a change in phase.

Under the most unfavorable circumstances, each field scattered from each scattering point exits the coil and aligns coherently and in phase with the source fields. This leads to inaccurate rotation rate measurements. One potential solution is to use wideband light sources. These sources have shorter coherent lengths, usually measured in microns. Because the coherence length is inversely proportional to the linewidth of the light source, using broadband light sources does not necessarily reduce backscattered power. However, it efficiently keeps the backscattered light from coherently interfering with the primary two beams. This prevents backscattered light from considerably influencing the phase shift between counter-propagating waves [76–78].

4.2.2.3.2. *Faraday Effect*, to achieve "full contrast" in an interferometer system, the two beams must have identical polarization states when they reach the detector. This state guarantees optimal interference. When the polarization states of the interfering waves are only partially matching, the

contrast of the interference pattern decreases. Furthermore, if their polarization states are totally orthogonal, no interference occurs. In FOGs, the Faraday effect is a rotation of optical polarization in a fiber loop that is magnetically induced due to the effect of a magnetic field gradient, as illustrated in figure 8 [79]. At the output detector, this effect is indistinguishable from Sagnac phase shift [7,39].

Several strategies exist to reduce this effect. Magnetic shielding, the use of polarization-maintain optical fiber, and actively managing the state of polarization within the fiber using a polarizer and polarization-preserving fibers all work together to form a polarization filter. Furthermore, using longer wavelengths can reduce the Faraday Effect by a factor of three to four. Another technique for reducing the Faraday Effect in fiber optic Gyroscope scopes is to use a depolarizer in a single-mode configuration [80–82].

$$\beta = V \cdot B \cdot d \tag{13}$$

where β is the amount of faraday rotation of the polarization state, Vis Verdet constant of the medium, B is the magnetic field and d is the fiber length.

The verdet constant V has λ^{-2} wavelength dependance it's equals for silica fiber to 2 rad T^{-1} m^{-1} at 850nm and 0.6 rad T^{-1} m^{-1} at 1550 nm wavelengths [2]. The total phase shift between the counter propagating waves due to Faraday Effect equals to [7]

$$\Delta\varphi = 2 * V \cdot B \cdot d \tag{14}$$

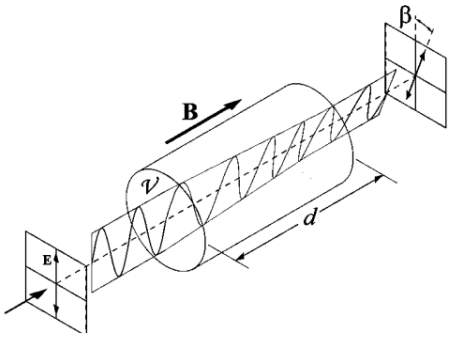

Figure 8. The Faraday Effect on polarization state

4.2.2.3.3. *Kerr effect*. Also known as the Quadratic Electro-Optic effect (QEO effect), was discovered in 1875 by Scottish physicist John Kerr. This phenomenon illustrates how a material's refractive index changes when exposed to an electrical field. The change in refractive index caused by the Kerr Effect is proportional to the square of the electric field i.e. the beam intensity.

The optical Kerr effect observed in optical fibers causes non-reciprocity that is regulated by light intensity. At greater optical intensities, the propagation characteristics of waves flowing in opposite directions become intensity-dependent. This nonlinearity, similar to four-wave mixing, has proven useful in nonlinear spectroscopy. Specifically, when these counter propagating waves have different strengths, their propagation properties diverge, resulting in a non-reciprocal phase shift similar to the Sagnac Effect. To address this, using broadband light sources such as super-luminescent LEDs with broad frequency spectrums is beneficial. When the Kerr Effect's phase shifts are averaged throughout a broadband source's wavelength components, the induced phase shift equals zero [83,84].

4.2.2.3.4. *Thermal effects [Shupe effect*]. Reciprocity within FOG is only reliable if the optical paths of both counter-propagating beams is kept stable throughout time. Thermal perturbations in a fiber are commonly known to cause changes in the fiber's propagation phase. This is due to the direct correlation of fiber length and refractive index with temperature, as well as strain-induced changes in the refractive index caused by the fiber core, cladding, and jacket's different thermal expansion coefficients.

As each counter-propagating field travels the same parts of the fiber at different times, dynamic and non-uniform variations along the coil's length caused fluctuations in the relative phase of the two counter-propagating beams. These phase irregularities cause differences in the sensor's output power. Shupe was the first to measure the error in a FOG due to this phenomenon [85–87].

Indeed, there are ways to handle this issue. One method involves using a fiber with a low refractive-index temperature coefficient. Another option is to arrange the fiber coil so that segments equidistant from the coil's center are next to one another. To decrease thermal impacts, two well-established winding techniques have been developed: bipolar and quadripolar winding. In both methods, the fiber coil is twisted from the center, alternating layers from each half-coil.

Absolutely, the different limits of Gyroscope can add errors, resulting in inequalities between phase shifts caused by rotation rate (known as the Sagnac effect) and other interfering factors. These differences can suppress or interfere with the predicted phase shift due to the rotation rate. This discrepancy in phase shifts has been a significant challenge, explaining why it took researchers so long to convert the Gyroscope from the research phase to the implementation stage [7].

4.2.2.3.5*. Scale Factor Errors.* As mentioned before sensor issues are caused by phase errors, which generate output power variations that are similar to those caused by rotation. Another cause of output power fluctuations is instabilities in the Gyroscope 's scale factor. Scale factor is the relation between phase shift and rotation rate as mentioned at equation 11, so any change of scale factor leads to the phase shift change consequently, detected power change.

$$SF = \frac{2\pi LD}{\lambda C} \tag{15}$$

A Gyroscope as rotation rate sensor is used in inertial navigation to construct an accurate pointing device by integrating its output over time. Tiny inaccuracies in the scale factor can accumulate over time and cause significant attitude issues. Scale factor instabilities can be either due to the fiber coil itself, which can introduce instability in loop length L or loop diameter D. Or due to the light source, which may have instabilities in mean wavelength λ. For common inertial navigation applications, these parameters should be stabilized to 1-ppm accuracy [39,88].

Temperature and acoustic changes cause fluctuations in coil size. Proper coil housing requires efficient thermal and acoustic isolation. High-end FOG suffer from scale factor instabilities caused by thermal instability in the mean wavelength of broad-band sources. FOG technology still falls below RLG technology in terms of scale factor instability, which is a key performance criterion. Using a laser diode instead of broad band light sources is the solution of this error.

As a summary, both RLGs and FOGs have shown that they can work in harsh environments where mechanical devices would have problems. Both are still making progress in areas that mechanical devices used to be the only ones that can operate. Additionally, there are also RLGs that can perform much better than what is needed for many applications, but they are too expensive and need high power to operate. Knowing that with the current fiber technology improvement rate, it may be possible to make FOGs that perform more effectively and even can win out over RLG technology. FOGs and MEMS Gyroscope technologies will be used in a similar way because MEMS have a lot of benefits, like being smaller, using less power, and being cheaper. The technology of MEMS is almost ready to

move on to the next stage of performance. As of now, MEMS's bias stability (around 5 to 30/h) doesn't meet the requirements for tactical grade, even though they might be able to compete with tactical RLGs and FOGs. Right now, MEMS Gyroscopes are very advanced in their growth, which means they will soon be able to replace Optical Gyroscopes.[4]

For evaluating different types of Gyroscopes, we took several parameters to point out which Gyroscope type is better. For Cost, size, life time and flexibility of packaging, FOGs and MEMS are cheaper, smaller in size, long life and have more flexible in packaging than both RLGs and Mechanical Gyroscopes. While, in turn on time and dynamic range, FOGs and RLGs are faster and wider in dynamic range than both MEMS and Mechanical Gyroscopes.

Also, we divided Gyroscopes technology with respect to bias stability into those with bias stability between 0.0001:0.01 deg/h which fits the strategic performance grade, FOGs and RLGs are the most suitable Gyroscopes. And, those with bias stability value between 0.01:0.1 deg/h which fits the navigation systems performance grade, FOGs and RLGs are the most suitable Gyroscopes can be used. Gyroscopes with bias stability value between 0.1:1 deg/h which fits the high-end tactical performance grade applications, FOGs and RLGs are the most suitable used Gyroscopes. At a bias stability value between 0.1:30 deg/h which fits the tactical Performance grade applications, FOGs and RLGs are the most suitable used Gyroscopes. Bias stability value between 1:30 deg/h which fits the industrial Performance grade applications, MEMS Gyroscope scopes are the most suitable used Gyroscopes. Finally, those with a bias stability value between 30:1000 deg/h which fits the consumer Performance grade applications, MEMS Gyroscope scopes are the most suitable used Gyroscopes.[4]

5. Conclusion

Our present work goes through the Gyroscope technologies that became now a days more popular than before due to the high demand of Gyroscope as one of the main and most important building blocks of many technologies. The Gyroscopes that we reviewed are Mechanical Gyroscope, Optical Gyroscope and MEMS Gyroscope on both large and small scales. Focusing on the main features, performances and technologies. Especially FOGs due to their superiority over other types of Gyroscopes in cost and size and power. At the early years of the invention of FOGs they were only used in non-accurate applications from 10 degrees per hour to 100 degrees per hour, but now a days they are also used in accurate applications up to 0.001 degrees per hour and are a strong competitor to RLGs.

In summary, our review comprehensively examines gyroscopes, detailing their types, characteristics, and limitations. We contribute by synthesizing existing research, offering insights into current trends and gaps in knowledge, and highlighting the practical implications of gyroscopic technology. By doing so, we aim to drive further advancements and innovation in gyroscopic systems and their applications

Future research in the realm of fiber optic gyroscopes could focus on enhancing their precision and sensitivity to meet evolving navigational demands. Exploring novel materials and designs, optimizing signal processing algorithms, and integrating advanced calibration techniques could further improve the performance and reliability of fiber optic gyroscopes in various applications. Additionally, investigating miniaturization and cost-effective manufacturing processes would broaden their accessibility and integration into diverse technological platforms

6. References

[1] Titterton D and Weston J L 2004 *Strapdown inertial navigation technology* vol 17 (IET)

[2] Lloyd S W 2014 *Improving fiber optic gyroscope performance using a single-frequency laser* (Stanford University)

[3] King A D 1998 Inertial navigation-forty years of evolution *GEC review* **13** 140–9

[4] Passaro V M N, Cuccovillo A, Vaiani L, De Carlo M and Campanella C E 2017 Gyroscope technology and applications: A review in the industrial perspective *Sensors* **17** 2284

[5] Nayak J 2011 Fiber-optic gyroscopes: from design to production *Appl Opt* **50** E152–61

[6] Aronowitz F 1971 The laser gyro *Laser applications*

[7] Lefevre H C 2022 *The fiber-optic gyroscope* (Artech house)

[8] Greiff P, Boxenhorn B, King T and Niles L 1991 Silicon monolithic micromechanical gyroscope *TRANSDUCERS'91: 1991 International Conference on Solid-State Sensors and Actuators. Digest of Technical Papers* (IEEE) pp 966–8

[9] Merlo M N and Donati S 2000 Handbook of Fibre Optic Sensing Technology *López-Higuera, JM, Session* **16**

[10] Eshtewi M M H and Malek H M A Gyroscope Technologies: An Effective Role in the Mechanical & Optical Perspective

[11] Tanaka T, Igarashi Y, Nara M and Yoshino T 1994 Automatic north sensor using a fiber-optic gyroscope *Appl Opt* **33** 120–3

[12] Zheng J 2005 All-fiber single-mode fiber frequency-modulated continuous-wave Sagnac gyroscope *Opt Lett* **30** 17–9

[13] Burns W K 1998 Fiber optic gyroscopes-light is better *Opt Photonics News* **9** 28–32

[14] Greiff P, Antkowiak B, Campbell J and Petrovich A 1996 Vibrating wheel micromechanical gyro *Proceedings of Position, Location and Navigation Symposium-PLANS'96* (IEEE) pp 31–7

[15] Maenaka K, Fujita T, Konishi Y and Maeda M 1996 Analysis of a highly sensitive silicon gyroscope with cantilever beam as vibrating mass *Sens Actuators A Phys* **54** 568–73

[16] Armenise M N, Ciminelli C, De Leonardis F, Diana R, Passaro V and Peluso F 2003 Gyroscope technologies for space applications *Optoelectronics Laboratory, Dipartimento di Elettrotecnica ed Elettronica, Politecnico di Bari* **6**

[17] Thielman L O, Bennett S, Barker C H and Ash M E 2002 Proposed IEEE Coriolis Vibratory Gyro standard and other inertial sensor standards *2002 IEEE Position Location and Navigation Symposium (IEEE Cat. No. 02CH37284)* (IEEE) pp 351–8

[18] Geiger W, Folkmer B, Merz J, Sandmaier H and Lang W 1999 A new silicon rate gyroscope *Sens Actuators A Phys* **73** 45–51

[19] Geiger W, Butt W U, Gaisser A, Frech J, Braxmaier M, Link T, Kohne A, Nommensen P, Sandmaier H and Lang W 2002 Decoupled microgyros and the design principle DAVED *Sens Actuators A Phys* **95** 239–49

[20] Clark W A, Howe R T and Horowitz R 1996 Surface micromachined Z-axis vibratory rate gyroscope *Tech. Dig. Solid-state sensor and actuator workshop* pp 283–7

[21] Zhanshe G, Fucheng C, Boyu L, Le C, Chao L and Ke S 2015 Research development of silicon MEMS gyroscopes: A review *Microsystem Technologies* **21** 2053–66

[22] Zaman M F, Sharma A and Ayazi F 2006 High performance matched-mode tuning fork gyroscope *19th IEEE International Conference on Micro Electro Mechanical Systems* (IEEE) pp 66–9

[23] Xia D, Yu C and Kong L 2014 The development of micromachined gyroscope structure and circuitry technology *Sensors* **14** 1394–473

[24] Trusov A A, Schofield A R and Shkel A M 2011 Micromachined rate gyroscope architecture with ultra-high quality factor and improved mode ordering *Sens Actuators A Phys* **165** 26–34

[25] Wang R, Cheng P, Xie F, Young D and Hao Z 2011 A multiple-beam tuning-fork gyroscope with high quality factors *Sens Actuators A Phys* **166** 22–33

[26] Tsai C-W, Chen K, Shen C-K and Tsai J 2011 A MEMS doubly decoupled gyroscope with wide driving frequency range *IEEE Transactions on Industrial Electronics* **59** 4921–9

[27] Pyatishev E N, Enns Y B, Kazakin A N, Kleimanov R V, Korshunov A V and Nikitin N Y 2017 MEMS GYRO comb-shaped drive with enlarged capacity gradient *2017 24th Saint Petersburg International Conference on Integrated Navigation Systems (ICINS)* (IEEE) pp 1–3

[28] Post E J 1967 Sagnac effect *Rev Mod Phys* **39** 475

[29] Nuttall J D 1987 Optical gyroscopes *Electronics and Power* **33** 703–7

[30] Juang J-N and Radharamanan R 2009 Evaluation of ring laser and fiber optic gyroscope technology *School Of Engineering, Mercer University, Macon, GA* **31207** 1–9

[31] Andronova I A and Malykin G B 2002 Physical problems of fiber gyroscopy based on the Sagnac effect *Physics-Uspekhi* **45** 793

[32] Kintner E C 1981 Polarization control in optical-fiber gyroscopes *Opt Lett* **6** 154–6

[33] Khoshki R M and Ganesan S 2014 Investigation on Closed-loop Fiber Optic Gyroscope Structure and Operation *International Journal of Hybrid Information Technology* **7** 23–32

[34] Shen C and Chen X 2012 Analysis and modeling for fiber-optic gyroscope scale factor based on environment temperature *Appl Opt* **51** 2541–7

[35] Ashby N 2004 The sagnac effect in the global positioning system *Relativity in rotating frames: relativistic physics in rotating reference frames* (Springer) pp 11–28

[36] Malykin G B 2000 The Sagnac effect: correct and incorrect explanations *Physics-Uspekhi* **43** 1229

[37] Tartaglia A and Ruggiero M L 2015 The Sagnac effect and pure geometry *Am J Phys* **83** 427–32

[38] Arditty H J and Lefevre H C 1981 Sagnac effect in fiber gyroscopes *Opt Lett* **6** 401–3

[39] Bergh R, Lefevre H and Shaw H 1984 An overview of fiber-optic gyroscopes *Journal of Lightwave Technology* **2** 91–107

[40] Korkishko Y N, Fedorov V A, Prilutskii V E, Ponomarev V G, Morev I V and Kostritskii S M 2012 Interferometric closed-loop fiber-optic gyroscopes *Third Asia Pacific Optical Sensors Conference* vol 8351 (SPIE) pp 810–7

[41] Wang R, Zheng Y and Yao A 2004 Generalized sagnac effect *Phys Rev Lett* **93** 143901

[42] Liu R Y and Adams G W 1990 Interferometric fiber-optic gyroscopes: a summary of progress *IEEE Symposium on Position Location and Navigation. A Decade of Excellence in the Navigation Sciences* (IEEE) pp 31–5

[43] Loukianov D 1999 *Optical gyros and their application* vol 9 (North Atlantic Treaty Organization Resear Rganization)

[44] Su C-C 2001 On the Sagnac effect in wave propagation *J Electromagn Waves Appl* **15** 945–55

[45] Fizeau M H 1991 Sur les hypothèses relatives à l'éther lumineux, et sur une expérience qui parait démontrer que le mouvement des corps change la vitesse avec laquelle la lumière se propage dans leur intérieur *SPIE milestone series* **28** 445–9

[46] LEFÈRE H C 1997 Fundamentals of the interferometric fiber-optic gyroscope *Opt Rev* **4** 20–7

[47] Skalský M, Havránek Z and Fialka J 2019 Efficient modulation and processing method for closed-loop fiber optic gyroscope with piezoelectric modulator *Sensors* **19** 1710

[48] Pavlath G A 2012 Fiber optic gyros past, present, and future *OFS2012 22nd International Conference on Optical Fiber Sensors* vol 8421 (SPIE) pp 53–62

[49] Stedman G E 1997 Ring-laser tests of fundamental physics and geophysics *Reports on progress in physics* **60** 615

[50] Pavlath G A 1994 Fiber-optic gyroscopes *Proceedings of LEOS'94* vol 2 (IEEE) pp 237–8

[51] Napolitano F 2010 Fiber-optic gyroscopes key technological advantages *IXSEA Newsletter*

[52] Hotate K 1990 Noise sources and countermeasures in optical passive ring-resonator gyro *Optical Fibre Sensors Conference (7th, 1990: Sydney, NSW)* (The Institution of Radio and Electronics Engineers Australia Edgecliff, NSW) pp 11–7

[53] Lefevre H C 2012 The fiber-optic gyroscope: actually better than the ring-laser gyroscope? *OFS2012 22nd International Conference on Optical Fiber Sensors* vol 8421 (SPIE) pp 63–70

[54] Tajmar M, Plesescu F and Seifert B 2009 Anomalous fiber optic gyroscope signals observed above spinning rings at low temperature *Journal of Physics: Conference Series* vol 150 (IOP Publishing) p 032101

[55] Apotin V S 2015 Ring Laser Gyroscope and Their Uses *Космическое приборостроение: сборник научных трудов III Всероссийского форума школьников, студентов, аспирантов и молодых ученых с международным участием, г. Томск, 8-10 апреля 2015 г.* 271–5

[56] Mignot A, Feugnet G, Schwartz S, Sagnes I, Garnache A, Fabre C and Pocholle J-P 2009 Single-frequency external-cavity semiconductor ring-laser gyroscope *Opt Lett* **34** 97–9

[57] Schwartz S, Gutty F, Feugnet G, Loil É and Pocholle J-P 2009 Solid-state ring laser gyro behaving like its helium-neon counterpart at low rotation rates *Opt Lett* **34** 3884–6

[58] Fan Z, Luo H, Lu G and Hu S 2012 Direct dither control without external feedback for ring laser gyro *Opt Laser Technol* **44** 767–70

[59] Korth W Z, Heptonstall A, Hall E D, Arai K, Gustafson E K and Adhikari R X 2016 Passive, free-space heterodyne laser gyroscope *Class Quantum Gravity* **33** 035004

[60] Hurst R B, Mayerbacher M, Gebauer A, Schreiber K U and Wells J-P R 2017 High-accuracy absolute rotation rate measurements with a large ring laser gyro: establishing the scale factor *Appl Opt* **56** 1124–30

[61] Hotate K 1997 Future evolution of fiber optic gyros *Opt Rev* **4** 28–34

[62] Morrow R B and Heckman D W 1996 High precision IFOG insertion into the strategic submarine navigation system *IEEE 1998 Position Location and Navigation Symposium (Cat. No. 98CH36153)* (IEEE) pp 332–8

[63] Wysocki P F, Digonnet M J F, Kim B Y and Shaw H J 1992 Broadband fiber sources for gyros *Fiber Optic Gyros: 15th Anniversary Conf* vol 1585 (SPIE) pp 371–82

[64] Burns W and Moeller R 1984 Polarizer requirements for fiber gyroscopes with high-birefringence fiber and broad-band sources *Journal of lightwave technology* **2** 430–5

[65] Heckman D W and Baretela M 2000 Interferometric fiber optic gyro technology (IFOG) *IEEE Aerospace and Electronic Systems Magazine* **15** 23–8

[66] Armenise M N, Ciminelli C, Dell'Olio F and Passaro V M N 2010 *Advances in gyroscope technologies* (Springer Science & Business Media)

[67] Honthaas J, Buret T, Paturel Y and Gaiffe T 2006 High Performance FOG: one design, no limit yet!? *Optical Fiber Sensors* (Optica Publishing Group) p ME3

[68] Udd E and Cahill R F 1979 Phase-nulling fiber-optic laser gyro *Opt. Lett* **4** 93–5

[69] Lefevre H C, Bettini J P, Vatoux S and Papuchon M 1986 Progress in optical fiber gyroscopes using integrated optics *In AGARD Guided Optical Structures in the Military Environment 13 p (SEE N87-13273 04-74*

[70] Çelikel O 2007 Construction and characterization of interferometric fiber optic gyroscope (IFOG) with erbium doped fiber amplifier (EDFA) *Opt Quantum Electron* **39** 147–56

[71] Yu Q, Li X and Zhou G 2009 A kind of hybrid optical structure IFOG *2009 International Conference on Mechatronics and Automation* (IEEE) pp 5030–4

[72] Lloyd S W, Fan S and Digonnet M J F 2013 Experimental observation of low noise and low drift in a laser-driven fiber optic gyroscope *Journal of Lightwave Technology* **31** 2079–85

[73] Ma H, Wang W, Ren Y and Jin Z 2012 Low-noise low-delay digital signal processor for resonant micro optic gyro *IEEE Photonics Technology Letters* **25** 198–201

[74] Lei M, Feng L, Zhi Y, Liu H, Wang J, Ren X and Su N 2013 Current modulation technique used in resonator micro-optic gyro *Appl Opt* **52** 307–13

[75] Wang Z, Yang Y, Lu P, Luo R, Li Y, Zhao D, Peng C and Li Z 2014 Dual-polarization interferometric fiber-optic gyroscope with an ultra-simple configuration *Opt Lett* **39** 2463–6

[76] Nakazawa M 1983 Rayleigh backscattering theory for single-mode optical fibers *JOSA* **73** 1175–80

[77] Marcuse D 2013 *Theory of dielectric optical waveguides* (Elsevier)

[78] Skorobogatiy M, Jacobs S A, Johnson S G and Fink Y 2002 Geometric variations in high index-contrast waveguides, coupled mode theory in curvilinear coordinates *Opt Express* **10** 1227–43

[79] Sağlar İ F 2007 *Interferometric Fiber Optic Gyroscope*

[80] Böhm K, Petermann K and Weidel E 1982 Sensitivity of a fiber-optic gyroscope to environmental magnetic fields *Opt Lett* **7** 180–2

[81] Hotate K and Tabe K 1986 Drift of an optical fiber gyroscope caused by the Faraday effect: influence of the earth's magnetic field *Appl Opt* **25** 1086–92

[82] Wen H, Terrel M A, Kim H K, Digonnet M J F and Fan S 2009 Measurements of the birefringence and Verdet constant in an air-core fiber *Journal of Lightwave Technology* **27** 3194–201

[83] Petermann K 1982 Intensity-dependent nonreciprocal phase shift in fiber-optic gyroscopes for light sources with low coherence *Opt Lett* **7** 623–5

[84] Shore K A 2012 Fiber Optics: Physics and Technology, by Fedor Mitschke: Scope: manual. Level: advanced undergraduate and postgraduate

[85] Frigo N J 1983 Compensation of linear sources of non-reciprocity in Sagnac interferometers *Fiber Optic and Laser Sensors I* vol 412 (SPIE) pp 268–71

[86] Shupe D M 1980 Thermally induced nonreciprocity in the fiber-optic interferometer *Appl Opt* **19** 654–5

[87] Ling W, Li X, Xu Z, Zhang Z and Wei Y 2015 Thermal effects of fiber sensing coils in different winding pattern considering both thermal gradient and thermal stress *Opt Commun* **356** 290–5

[88] Liu R-Y, El-Wailly T F and Dankwort R C 1992 Test results of Honeywell's first-generation high-performance interferometric fiber optic gyroscope *Fiber Optic Gyros: 15th Anniversary Conf* vol 1585 (SPIE) pp 262–75